Finite Width of Anyons Changes Their Braiding Signature

K. Iyer,* F. Ronetti, B. Grémaud, T. Martin, J. Rech, and T. Jonckheere
Aix Marseille Univ, Université de Toulon, CNRS, CPT, Marseille, France

(Received 25 November 2023; revised 12 March 2024; accepted 9 April 2024; published 21 May 2024)

Anyons are particles intermediate between fermions and bosons, characterized by a nontrivial exchange phase, yielding remarkable braiding statistics. Recent experiments have shown that anyonic braiding has observable consequences on edge transport in the fractional quantum Hall effect (FQHE). Here, we study transport signatures of anyonic braiding when the anyons have a finite width. We show that the width of the anyons, even when extremely small, can have a tremendous impact on transport properties and braiding signatures. In particular, we find that taking the finite width into account allows us to explain recent experimental results on the FQHE at filling factor $2/5$ [M. Ruelle *et al.*, Phys. Rev. X **13**, 011031 (2023)]. Our work shows that the finite width of anyons crucially influences setups involving anyonic braiding, especially when the exchange phase is larger than $\pi/2$.

DOI: 10.1103/PhysRevLett.132.216601

Anyons are particles intermediate between bosons and fermions, characterized by fractional exchange statistics [1–3]. These are proposed to occur in two spatial dimensions, and have found a solid experimental footing in the fractional quantum Hall effect (FQHE) [4,5]. Fundamental interest and potential technological applications [6] have fueled intense activity leading to several theoretical proposals to detect anyonic statistics in the FQHE [7–15]. Only recently, experiments were able to detect anyonic statistics in the FQHE in the simplest filling fraction of $1/3$ [16–19] as well as in the more complicated fraction of $2/5$ [20–22].

Transport experiments on FQHE edges have been successful in quantitatively extracting anyonic statistics by measuring current correlations. In contrast to spatial braiding as in the Fabry-Perot geometries, the physical mechanism at play here is time-domain braiding [23]. In the latter, anyons emitted from a source quantum point contact (QPC) form a braiding loop in time with anyon pairs excited at a QPC in the FQHE. The braiding loop in time is due to the interference between two different time-ordered processes [24,25].

Experiments are well captured by the theoretical formalism for $\nu = 1/3$ FQHE where the exchange phase is $\pi/3$ [26]. However, experimental results at $\nu = 2/5$, where theory predicts an exchange phase of $3\pi/5$, strongly differ from the theoretical predictions, even for a quantity as essential as the sign of the tunneling current. The multiedge structure of the $\nu = 2/5$ FQHE suggests the influence of interedge interactions or edge reconstruction, among others, as possible sources of the observed deviation from theoretical predictions. However, none of these candidates seem to explain the observed sign of the tunneling current.

In existing calculations, the natural assumption is to neglect the width of anyons. Indeed, while anyonic excitations always have a nonzero extension, it is deemed negligible as it is typically much smaller than the average spacing between successive anyons, and the thermal length of the system. In this Letter, we show that the finite width of the anyons, even when small, significantly affects their braiding signatures, reflecting on the transport properties of the system, in particular for composite fractions of the FQHE where the exchange phase is larger than $\pi/2$. Beyond the specific system we consider, our results show that the finite extension of anyons is an essential ingredient for a correct description of setups involving anyonic braiding.

Time-domain braiding.—We first review the basics of time-domain anyonic braiding [15,23,24,27]. Consider the geometry of Fig. 1, showing a Hall bar in the FQHE with chiral edge states, equipped with a QPC operating in the weak tunneling regime, where tunneling of quasiparticles between the edges can occur. For the system at equilibrium, at all times, spontaneous processes where a quasiparticle-quasihole (QP-QH) pair is created at the QPC do exist, leading to zero net current due to electron-hole symmetry. However, when a single quasiparticle (QP) on the upper edge impinges on the QPC, there is a nontrivial interference between the process where the QP-QH pair is created before, and the one where it is created after the arrival of the single QP. The interference of these two processes leads to a braiding loop in the time domain, with an overall coefficient $1 - e^{2i\theta}$, where θ is the exchange phase between two QPs. For fermions and bosons, the overall contribution is zero, as $\theta = \pi$ or 0, and the tunneling current is only due to direct tunneling of the incoming QP through the QPC. For anyons however, the cancellation is only partial due to their nontrivial braiding statistics, with for example $\theta = \pi/3$ for anyonic QPs in $\nu = 1/3$ FQHE. It has been shown that this anyonic exchange dominantly contributes

to physically measurable quantities at the QPC such as the average tunneling current and current correlations [24,25]. In this work, we consider the impact of the finite width of the incoming QP on the anyonic exchange process, and its consequences on the transport properties.

Model.—We consider a Hall bar in the FQHE with chiral edge states, equipped with a QPC where tunneling between the edge states can occur (see Fig. 1). For simplicity, each edge is described as a single mode Laughlin chiral Luttinger liquid. As shown in the Supplemental Material [28], this can capture the physics of complex composite fractions like $\nu = 2/5$ by adapting the values of the parameters [see the discussion of Eq. (3)]. Up and down edge states are described in the total Hamiltonian as $H_{0u/d} = (v_F/4\pi)\int dx(\partial_x\phi^{u/d})^2$, where ϕ^u (ϕ^d) denotes the bosonic mode on the upper (lower) edge, $v_F > 0$ is the propagation velocity of the bosonic mode. The bosonic modes satisfy equal-time commutation relations $[\phi^{u/d}(x), \phi^{u/d}(y)] = \pm i\pi \mathrm{sign}(x-y)$. The edge hosts anyonic quasiparticles of charge $e^* = \nu e$, described by the operator $\psi \sim e^{i\sqrt{\nu}\phi}$. The QPC is placed in the weak backscattering regime, causing tunneling of anyonic QPs between the two edges. The corresponding tunneling Hamiltonian is $H_T(t) = \Gamma[A(t) + A^\dagger(t)]$, where $A(t) = e^{i\sqrt{\nu}(\phi^u(0,t)-\phi^d(0,t))}$ and Γ is the tunneling amplitude. Similarly, the current flowing from edge u to d is given by $I_T(t) = ie^*\Gamma[A^\dagger(t) - A(t)]$.

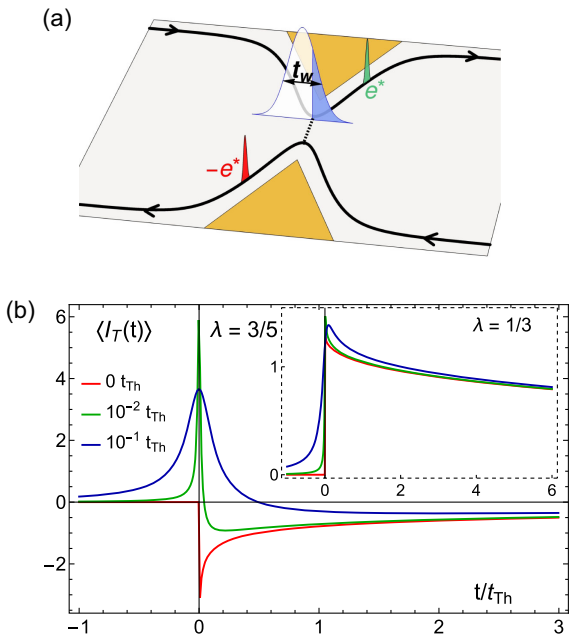

FIG. 1. (a) Idealized geometry of a FQHE bar with a QPC, showing an extended quasiparticle (QP, shape filled with blue and white) impinging on the QPC on the upper edge. A tunneling current through the QPC is created by the anyonic exchange between the QP and the QP-quasihole pairs (green-red) excited at the QPC. Because of its finite temporal width (t_w), the QP contributes only partially to braiding at time t at the QPC, as indicated by the blue part of the QP. (b) Tunneling current at the QPC, in units of $I_0 = \Gamma^2 T(\pi T\tau_0)^{2\delta-1}$, due to a single incoming QP as a function of time [Eq. (3)] for $\lambda = \delta = 3/5$, and for different QP widths ($t_w = 0$, 0.01, 0.1 in units of $t_{Th} = \hbar/k_BT$). The center of the QP hits the QPC at $t = 0$. As the width is increased the current shifts from negative to positive values. Inset: same figure for $\lambda = \delta = 1/3$, showing that the effect of the QP width is not significant for $\lambda < 1/2$.

Current due to a single QP.—We first consider the current created by a single anyonic QP on the upper edge incident on the QPC. Crucially, this QP is taken to have a finite extension. Because of chirality of the edge, this spatial width leads to a finite temporal width for the bosonic field at the position of the QPC. This can be modeled by adding a finite-width solitonic excitation on the bosonic edge modes [26,30]

$$\phi^u \longrightarrow \phi^u + 2\sqrt{\lambda}\left[\tan^{-1}\left(\frac{t-t_0}{t_w}\right) + \frac{\pi}{2}\right] \tag{1}$$

where t_w denotes the temporal width of the QP, whose center reaches the QPC at $t = t_0$ and $\pi\lambda$ is the phase due to the exchange of two QPs. The current at the QPC due to this QP can be expressed, to leading order in Γ, using the Keldysh formalism as [31]

$$\langle I_T(t)\rangle = -\frac{i}{2}\int dt' \sum_{\eta\eta'} \eta' \langle\{T_K I_T(t^\eta) H_T(t'^{\eta'})\}\rangle \tag{2}$$

where η, η' denote the Keldysh contour labels, and T_K denotes time ordering on the Keldysh contour. It takes the form [28]

$$\langle I_T(t)\rangle = 2ie^*\Gamma^2 \int_{-\infty}^{t} dt' \left(e^{2\delta\mathcal{G}(t-t')} - e^{2\delta\mathcal{G}(t'-t)}\right) \times \sin\left\{2\lambda\left[\tan^{-1}\left(\frac{t-t_0}{t_w}\right) - \tan^{-1}\left(\frac{t'-t_0}{t_w}\right)\right]\right\} \tag{3}$$

where $\mathcal{G}(t) = \langle T\phi(t)\phi(0)\rangle$ is the bosonic Green's function

$$\mathcal{G}(t) = \ln\left(\frac{\sinh(i\pi k_B T\tau_0/\hbar)}{\sinh[\pi k_B T(t - i\tau_0)/\hbar]}\right). \tag{4}$$

Here τ_0 is the short-time cutoff, T is the temperature, and δ is the scaling dimension of the QP tunneling across the QPC. For the Laughlin case, one simply has $\lambda = \delta = \nu$. For composite fractions, the values λ and δ can be adjusted to describe the physics of the associated QP. For example, for a FQHE with filling factor $\nu = 2/5$, the $e/5$ QPs can be addressed simply by taking $\lambda = \delta = 3/5$, and $e^* = e/5$, in Eq. (3) [28,32].

The incoming QP wave packet in Eq. (1) is assumed to have a Lorentzian profile [28]. Because of the finite width of the QP wave packet, its braiding phase is smeared in time, and it contributes only partially at a given time. This

can significantly affect the tunneling current as illustrated in Fig. 1(b). For $t_w \to 0$, the sine in Eq. (3) reduces to $\theta(t-t_0)\theta(t_0-t')\sin(2\pi\lambda)$, where θ is the Heaviside step function, the current then reduces to a slowly decaying function of time, with a characteristic timescale set by the temperature, $t_{\mathrm{Th}} = \hbar/(k_B T)$ [33].

We show the tunneling current as a function of time for $\lambda = 3/5$ in Fig. 1(b) for different values of the width t_w of the incoming QP, and $\delta = 3/5$. For $t_w = 0$, the tunneling current is strictly negative, as $\sin(2\pi \times 3/5) < 0$. As soon as the QP has a finite width, the current becomes positive, on a time interval around t_0 which becomes wider as t_w is increased. Importantly, even if δ is adjusted, the qualitative behavior of the currents remains largely unchanged, as long as $\lambda > 1/2$: changing δ modifies the power-law decrease of the Green functions in Eq. (3), which will mainly move the value of t_w at which the current becomes negative, without changing the overall behavior of the current. This behavior is in complete contrast to that at $\lambda = 1/3$ (which corresponds to the usual Laughlin $\nu = 1/3$ case). Here, the current due to a QP of zero width is positive. However, endowing the QP with a finite width does not significantly impact the current, as shown in the inset of Fig. 1, for $\delta = 1/3$. Again, the qualitative behavior is robust against a change of parameters, as long as $\lambda < 1/2$.

As shown in Fig. 1, the impact of a finite width is starkly different between $\lambda > 1/2$ and $\lambda < 1/2$. For $\lambda > 1/2$, the smearing of the braiding phase due to the finite width of the incoming anyon leads to an effective λ smaller than $1/2$ at small times, dramatically changing the sign of the current. On the other hand, for $\lambda < 1/2$, the smearing of the braiding phase only produces a small quantitative effect, without qualitative change of the current. $\lambda = 1/2$ acts as a threshold value: for $\lambda < 1/2$ (resp. $\lambda > 1/2$) the braiding at the QPC occurs dominantly between the incoming anyonic QP and the QPC QP (resp. QH), which explains why the tunneling current changes sign when λ crosses $1/2$ [28].

Poissonian stream of QPs.—We now consider the case of a Poissonian stream of QPs incident on the QPC, leading to an average current I_u (I_d) on the upper (lower) edge. This corresponds to the situation of Ref. [16] where upstream QPCs in the tunneling regime are used as the sources of the QP streams.

In the single QP case, there were two timescales characterizing the system: the thermal time $t_{Th} = \hbar/(k_B T)$ and, t_w, the temporal width of the QP. A stream of QPs introduces another important timescale: the average temporal spacing between successive QPs, given by the inverse of the incoming current on the QPC, $t_s = e^*/I_+$, where $I_\pm = I_u \pm I_d$.

Normalizing all times with t_s, the stream of incoming QPs on the QPC can be modeled by modifying the bosonic fields as

$$\phi^{u/d} \longrightarrow \phi^{u/d} + 2\sqrt{\lambda}\sum_k \left[\tan^{-1}\left(\frac{(t-t_k^{u/d})/t_s}{\tau_w}\right) + \frac{\pi}{2}\right] \quad (5)$$

where $t_k^{u/d}$ denotes the time at which the kth QP on the u/d edge hits the QPC, and these times follow a Poissonian distribution. Moreover, we have defined the scaled width of QPs, $\tau_w = t_w/t_s$. Using the expression of the current in Eq. (2), the average tunneling current at the QPC is [28]

$$\langle I_T \rangle = -4e^*\Gamma^2 \int_0^\infty dt \frac{\sin\left[x\mathrm{Im}f(t,\lambda,\tau_w)\right]}{\exp\left[\mathrm{Re}f(t,\lambda,\tau_w)\right]} \mathrm{Im}(e^{2\delta\mathcal{G}(t)}) \quad (6)$$

where we have performed a Poissonian average over the times $t_k^{u/d}$, and $x = I_-/I_+$ is the asymmetry of the incoming currents. $f(t,\lambda,\tau_w)$ is the phase accumulated as finite-width QPs pass the QPC, and is given by

$$f(t,\lambda,\tau_w) = \int_{-\infty}^{\infty} du \left\{1 - \exp\left(-2i\lambda\left[\tan^{-1}\left(\frac{t/t_s - u}{\tau_w}\right) + \tan^{-1}\left(\frac{u}{\tau_w}\right)\right]\right)\right\}. \quad (7)$$

Here, the integration over u is essential as due to their finite width, the QPs start affecting the QPC even before their center hits the QPC. We emphasize that Eq. (7) gives the phase accumulated due to braiding of the Poissonian stream of finite-width QPs with QP-QH pairs at the QPC. This is readily seen by taking $t_w \to 0$, giving $f(t,\lambda,\tau_w) \to t/t_s(1-e^{-2i\pi\lambda})$, which is the phase due to a stream of zero-width QPs [26].

We plot the imaginary part of the finite-width phase $f(t,\lambda,\tau_w)$ as a function of time in Fig. 2, for $\lambda = 3/5$ and different values of the scaled width τ_w. For $\tau_w = 0$, the imaginary part of the phase is simply linear in t, with a negative slope equal to $\sin(2\pi\lambda)$. As soon as the QPs have a finite width, we find a dramatic change occurring close to $t = 0$: $\mathrm{Im}f(t,\lambda,\tau_w)$ is initially positive, and takes a finite amount of time (set by τ_w) to become negative and eventually recover the same negative slope. This behavior

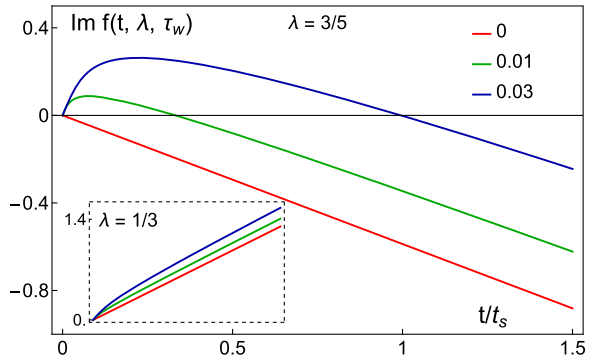

FIG. 2. Imaginary part of the finite-width phase as a function of time for $\lambda = 3/5$, for scaled width $\tau_w = 0,\ 0.01,\ 0.03$. It is $\sin(2\pi * 3/5)(t/t_s)$ for $\tau_w = 0$, but becomes positive close to $t = 0$ when τ_w is finite. Inset: same curves for $\lambda = 1/3$, showing that for $\lambda < 1/2$ a finite width does not significantly change the phase.

is reminiscent of the behavior of the current due to a single QP shown in Fig. 1. The inset of Fig. 2 shows the imaginary part of the phase for $\lambda = 1/3$. There, we see a linear behavior with a positive slope for $\tau_w = 0$, which is only marginally affected when τ_w is nonzero. Note that the real part of the phase, which also enters Eq. (6), mostly contributes to the integral at short times. However, it does not vary significantly with τ_w for any λ, and is thus not shown here.

Hence, close to $t = 0$, the effective phase experienced by the QPs tunneling across the QPC is quite different from the full phase of the QP. As the rest of the integrand is peaked close to $t = 0$, a sizable contribution to the tunneling current comes from the $t \simeq 0$ region. We find that this results in an average positive tunneling current for $\lambda = 3/5$, as opposed to a negative average tunneling current seen for delta-width QPs. This is shown in Fig. 3(a) where the mean current $\langle I_T \rangle$ is plotted as a function of the scaled width τ_w

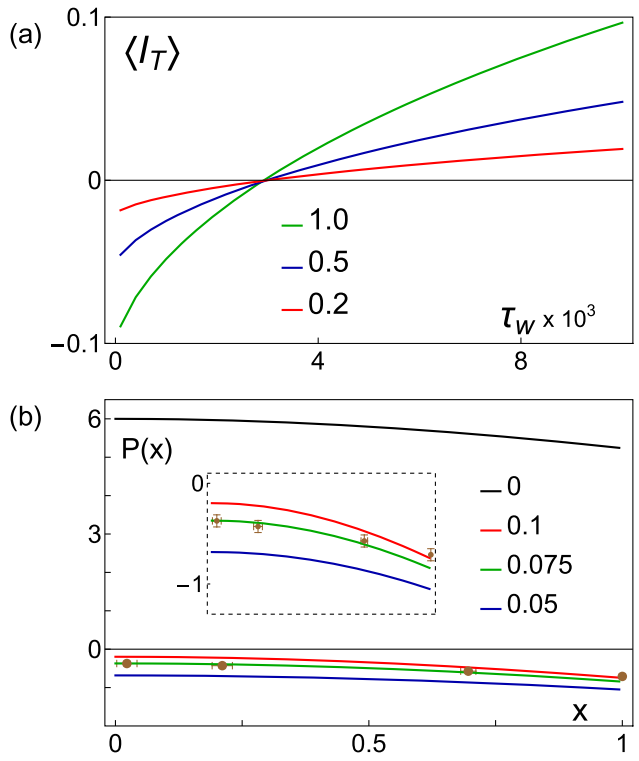

FIG. 3. (a) Tunneling current $\langle I_T \rangle$ at the QPC due to a stream of Poissonian QPs, as a function of scaled width τ_w, for different values of current asymmetry: $x = 0.2, 0.5, 1$. $\langle I_T \rangle$ is negative for very small τ_w, and becomes positive for $\tau_w \gtrsim 0.003$. (b) Fano factor $P(x)$ of Eq. (8) as a function of the current asymmetry x for different values of scaled width: $\tau_w = 0,\ 0.05,\ 0.075,\ 0.1$. Experimental data from Ref. [20] are shown as brown points with error bars. $P(x)$ is in contradiction even with the sign of the experimentally measured values for $\tau_w = 0$, but becomes compatible with the experimental data for $\tau_w \simeq 0.075$. Inset: enlargement of the region close to the experimental data points. Curves on both panels were obtained in the regime of negligible temperature.

for different values of the asymmetry x of the incoming currents. One readily sees that $\langle I_T \rangle$ grows from negative to positive as τ_w is increased. For Lorentzian QP wave packets, $\langle I_T \rangle$ changes sign at $\tau_w \sim 0.003$; for other shapes of finite width QPs (not shown), the qualitative behavior is the same.

We now examine the consequence of the finite width of the incoming QPs on the experimentally measured P factor [26,28], which is a generalized Fano factor for the cross-correlations of the output currents:

$$P(x = I_-/I_+) = \frac{\langle \delta I_u \delta I_d \rangle}{e^* I_+ \frac{\partial \langle I_T \rangle}{\partial I_-}\Big|_{I_-=0}} \tag{8}$$

where $\langle \delta I_u \delta I_d \rangle$ denotes the current cross-correlations. The P factor was measured in recent experiments [16,20,21] to extract anyonic statistics in the FQHE. For $\nu = 1/3$ FQHE, the experiments find an excellent agreement with the theory of Ref. [26] where the incoming QPs are assumed to have zero width. On the other hand, for $\nu = 2/5$, the experiments are in strong disagreement with the theoretical calculations, as the P factor is predicted to be positive and quite large (close to 6), while the experiments measure negative values of the order of -1.

We plot the P factor for $\nu = 2/5$ FQHE ($\lambda = 3/5$, $\delta = 3/5$) in Fig. 3(b) for different values of the scaled width τ_w. Experimental data points from Ref. [20] are shown in brown. The black curve denotes the predictions of Ref. [26] where $\tau_w = 0$, and is in complete disagreement with the experimental data. With a nonzero τ_w, the curves now have negative values, getting closer to the experimental data. The inset zooms into the region around the data points; we find that $\tau_w \sim 0.075$ agrees relatively well with the experiments.

The scaled width τ_w is proportional to the transparency $\mathcal{T}$ of the source QPCs. Indeed the applied voltage V before a source QPC can be seen as a regular stream of incoming excitations whose spacing is equal to their width ($\sim 1/V$). As only a fraction $\mathcal{T}$ of these excitations is transmitted, it gives a scaled width $\tau_w \sim \mathcal{T}$. The value $\tau_w \sim 0.075$ that we find to get a reasonable agreement with the experimental results for the P factor is thus compatible with the transparencies $\mathcal{T}$ used experimentally (typically $\mathcal{T} \sim 0.1$). A detailed comparison with experimental results, including the effect of varying the transparency $\mathcal{T}$ [18], and considering different shapes for the excitations [28], will be the subject of future work.

In conclusion, we have studied anyonic braiding signatures in FQHE edge transport accounting for the anyons' finite width. We have shown that the finite width of anyons decreases the effective braiding phase seen at the QPC. For a braiding phase $2\pi\lambda > \pi$, a finite width can lead to an effective phase $< \pi$, changing the sign of the tunneling current. This allows us to quantitatively explain recent

experiments on $\nu = 2/5$ FQHE. In contrast, for a braiding phase $2\pi\lambda < \pi$, the finite width only reduces this phase further, causing no change in the sign of tunneling current. This explains the relative insensitivity of $\nu = 1/3$ FQHE to the finite width of anyons. Our conclusions are robust against variation of the scaling dimension, which is typically nonuniversal.

This work naturally leads to several possible extensions. Given the crucial impact of the finite width of incoming anyons, it might be interesting to study the consequences of the finite extent of the QPC [34–36]. The impact of Coulomb interaction inside the QPC could also be important for a complete description of the system. Finally, accounting for the finite width may be important in other architectures involving anyons including flying qubits [37], Fabry-Perot, and Mach-Zehnder interferometry [38], and even in different physical platforms hosting anyons such as spin liquids [39–42].

Note added.—Recently, another work appeared [43], which also studies the impact of finite width on anyon colliders, and finds results consistent with ours.

We thank G. Fève and M. Ruelle for useful discussions, and for sharing their experimental data. We also thank M. Hashisaka and T. Kato for useful discussions. This work was carried out in the framework of the project "ANYHALL" (Grant ANR No. ANR-21-CE30-0064-03). It received support from the French government under the France 2030 investment plan, as part of the Initiative d'Excellence d'Aix-Marseille Université—A*MIDEX. We acknowledge support from the institutes IPhU (AMX-19-IET-008) and AMUtech (AMX-19-IET-01X).

*kishore.iyer@cpt.univ-mrs.fr

[1] J. M. Leinaas and J. Myrheim, Il Nuovo Cimento B (1971–1996) **37**, 1 (1977).
[2] F. Wilczek, Phys. Rev. Lett. **49**, 957 (1982).
[3] D. Arovas, J. R. Schrieffer, and F. Wilczek, Phys. Rev. Lett. **53**, 722 (1984).
[4] D. C. Tsui, H. L. Stormer, and A. C. Gossard, Phys. Rev. Lett. **48**, 1559 (1982).
[5] R. B. Laughlin, Phys. Rev. Lett. **50**, 1395 (1983).
[6] C. Nayak, S. H. Simon, A. Stern, M. Freedman, and S. Das Sarma, Rev. Mod. Phys. **80**, 1083 (2008).
[7] C. de C. Chamon, D. E. Freed, S. A. Kivelson, S. L. Sondhi, and X. G. Wen, Phys. Rev. B **55**, 2331 (1997).
[8] I. Safi, P. Devillard, and T. Martin, Phys. Rev. Lett. **86**, 4628 (2001).
[9] S. Vishveshwara, Phys. Rev. Lett. **91**, 196803 (2003).
[10] W. Bishara and C. Nayak, Phys. Rev. B **77**, 165302 (2008).
[11] G. Campagnano, O. Zilberberg, I. V. Gornyi, D. E. Feldman, A. C. Potter, and Y. Gefen, Phys. Rev. Lett. **109**, 106802 (2012).
[12] B. Rosenow and S. H. Simon, Phys. Rev. B **85**, 201302(R) (2012).
[13] I. P. Levkivskyi, J. Fröhlich, and E. V. Sukhorukov, Phys. Rev. B **86**, 245105 (2012).
[14] B. I. Halperin, A. Stern, I. Neder, and B. Rosenow, Phys. Rev. B **83**, 155440 (2011).
[15] B. Lee, C. Han, and H.-S. Sim, Phys. Rev. Lett. **123**, 016803 (2019).
[16] H. Bartolomei, M. Kumar, R. Bisognin, A. Marguerite, J.-M. Berroir, E. Bocquillon, B. Plaçais, A. Cavanna, Q. Dong, U. Gennser *et al.*, Science **368**, 173 (2020).
[17] J. Nakamura, S. Liang, G. C. Gardner, and M. J. Manfra, Nat. Phys. **16**, 931 (2020).
[18] J.-Y. M. Lee, C. Hong, T. Alkalay, N. Schiller, V. Umansky, M. Heiblum, Y. Oreg, and H.-S. Sim, Nature (London) **617**, 277 (2023).
[19] H. K. Kundu, S. Biswas, N. Ofek, V. Umansky, and M. Heiblum, Nat. Phys. **19**, 515 (2023).
[20] M. Ruelle, E. Frigerio, J.-M. Berroir, B. Plaçais, J. Rech, A. Cavanna, U. Gennser, Y. Jin, and G. Fève, Phys. Rev. X **13**, 011031 (2023).
[21] P. Glidic, O. Maillet, A. Aassime, C. Piquard, A. Cavanna, U. Gennser, Y. Jin, A. Anthore, and F. Pierre, Phys. Rev. X **13**, 011030 (2023).
[22] J. Nakamura, S. Liang, G. C. Gardner, and M. J. Manfra, Phys. Rev. X **13**, 041012 (2023).
[23] C. Han, J. Park, Y. Gefen, and H.-S. Sim, Nat. Commun. **7**, 11131 (2016).
[24] T. Morel, June-Young M. Lee, H.-S. Sim, and C. Mora, Phys. Rev. B **105**, 075433 (2022).
[25] J.-Y. M. Lee and H.-S. Sim, Nat. Commun. **13**, 6660 (2022).
[26] B. Rosenow, I. P. Levkivskyi, and B. I. Halperin, Phys. Rev. Lett. **116**, 156802 (2016).
[27] C. Mora, arXiv:2212.05123.
[28] See Supplemental Material at http://link.aps.org/supplemental/10.1103/PhysRevLett.132.216601 for details on the model with multiple bosonic edge modes [29], theory of the anyon collider, results for a different QP profile, and the relation between the braiding phase and the sign of the current.
[29] O. Shtanko, K. Snizhko, and V. Cheianov, Phys. Rev. B **89**, 125104 (2014).
[30] N. Schiller, Y. Shapira, A. Stern, and Y. Oreg, Phys. Rev. Lett. **131**, 186601 (2023).
[31] T. Martin, in *Nanophysics: Coherence and Transport*, Les Houches, Session LXXXI, edited by H. Bouchiat, Y. Gefen, S. Guéron, G. Montambaux, and J. Dalibard (Elsevier, New York, 2005), p. 283.
[32] X. G. Wen, Adv. Phys. **44**, 405 (1995).
[33] T. Jonckheere, J. Rech, B. Grémaud, and T. Martin, Phys. Rev. Lett. **130**, 186203 (2023).
[34] M. Aranzana, N. Regnault, and T. Jolicoeur, Phys. Rev. B **72**, 085318 (2005).
[35] D. Chevallier, J. Rech, T. Jonckheere, C. Wahl, and T. Martin, Phys. Rev. B **82**, 155318 (2010).
[36] L. Vannucci, F. Ronetti, G. Dolcetto, M. Carrega, and M. Sassetti, Phys. Rev. B **92**, 075446 (2015).
[37] D. C. Glattli, J. Nath, I. Taktak, P. Roulleau, C. Bauerle, and X. Waintal, arXiv:2002.03947.

[38] M. Carrega, L. Chirolli, S. Heun, and L. Sorba, Nat. Rev. Phys. **3**, 698 (2021).
[39] L. Savary and L. Balents, Rep. Prog. Phys. **80**, 016502 (2016).
[40] K. Klocke, D. Aasen, R. S. K. Mong, E. A. Demler, and J. Alicea, Phys. Rev. Lett. **126**, 177204 (2021).
[41] K. Klocke, J. E. Moore, J. Alicea, and G. B. Halász, Phys. Rev. X **12**, 011034 (2022).
[42] Y. Liu, K. Slagle, K. S. Burch, and J. Alicea, Phys. Rev. Lett. **129**, 037201 (2022).
[43] M. Thamm and B. Rosenow, arXiv:2312.04475.